RESEARCH ARTICLE

# Association of Structural Measurements of Brain Reserve With Motor Progression in Patients With Parkinson Disease

Linbo Wang, PhD,* Ping Wu, MD,* Peter Brown, MD, Wei Zhang, MSc, Fengtao Liu, MD, Yan Han, MD, Chuan-Tao Zuo, MD†, Wei Cheng, PhD†, and Jianfeng Feng, PhD†

**Correspondence**
Dr. Feng
jffeng@fudan.edu.cn

*Neurology*® 2022;99:e977-e988. doi:10.1212/WNL.0000000000200814

## Abstract

### Background and Objectives

To investigate the relationship between baseline structural measurements of brain reserve and clinical progression in Parkinson disease (PD). To further provide a possible underlying mechanism for structural measurements of brain reserve in PD, we combined functional and transcriptional data and investigated their relationship with progression-associated patterns derived from structural measurements and longitudinal clinical scores.

### Methods

This longitudinal study collected data from June 2010 to March 2019 from 2 datasets. The Parkinson's Progression Markers Initiative (PPMI) included controls and patients with newly diagnosed PD from 24 participating sites worldwide. Results were confirmed using data from the Huashan dataset (Shanghai, China), which included controls and patients with PD. Clinical symptoms were assessed with Movement Disorder Society–sponsored revision of the Unified Parkinson's Disease Rating Scale (MDS-UPDRS) scores and Schwab & England activities of daily living (ADL). Both datasets were followed up to 5 years. Linear mixed-effects (LME) models were performed to examine whether changes in clinical scores over time differed as a function of brain structural measurements at baseline.

### Results

A total of 389 patients with PD (n = 346, age 61.3 ± 10.03, 35% female, PPMI dataset; n = 43, age 59.4 ± 7.3, 38.7% female, Huashan dataset) with T1-MRI and follow-up clinical assessments were included in this study. Results of LME models revealed significant interactions between baseline structural measurements of subcortical regions and time on longitudinal deterioration of clinical scores (MDS-UPDRS Part II, absolute $\beta > 0.27$; total MDS-UPDRS scores, absolute $\beta > 1.05$; postural instability–gait difficulty (PIGD) score, absolute $\beta > 0.03$; Schwab & England ADL, absolute $\beta > 0.59$; all $p < 0.05$, false discovery rate corrected). The interaction of baseline structural measurements of subcortical regions and time on longitudinal deterioration of the PIGD score was replicated using data from Huashan Hospital. Furthermore, the β-coefficients of these interactions recapitulated the spatial distribution of dopaminergic, metabolic, and structural changes between patients with PD and normal controls and the spatial distribution of expression of the α-synuclein gene (*SNCA*).

*These authors contributed equally to the work

†These authors contributed equally to the work as co-senior authors.

From the Institute of Science and Technology for Brain-inspired Intelligence (L.W., W.Z., W.C., J.F.), Fudan University; Key Laboratory of Computational Neuroscience and Brain-Inspired Intelligence (Fudan University) (L.W., W.Z., W.C., J.F.), Ministry of Education; PET Center (P.W., C.-T.Z.), Huashan Hospital, Fudan University, Shanghai, China; Medical Research Council Brain Network Dynamics Unit (P.B.), and Nuffield Department of Clinical Neurosciences (P.B.), John Radcliffe Hospital, University of Oxford, United Kingdom; Department of Neurology (F.L., C.-T.Z.), Huashan Hospital North, Fudan University; Department of Neurology (Y.H.), Yueyang Hospital of Integrated Traditional Chinese and Western Medicine, Shanghai University of Traditional Chinese Medicine; Human Phenome Institute (C.-T.Z.), Fudan University; Zhangjiang Fudan International Innovation Center (W.C., J.F.), Shanghai, China; Department of Computer Science (W.C., J.F.), University of Warwick, Coventry, United Kingdom; and Fudan ISTBI—ZJNU Algorithm Centre for Brain-inspired Intelligence (W.C., J.F.), Zhejiang Normal University, Jinhua, China.

Go to Neurology.org/N for full disclosures. Funding information and disclosures deemed relevant by the authors, if any, are provided at the end of the article.

## Glossary

**$^{11}$C-CFT** = 2b-carbomethoxy-3b-(4-trimethylstannylphenyl) tropane; **$^{18}$F-FDG** = $^{18}$F-fluorodeoxyglucose; **ADL** = activities of daily living; **AHBA** = Allen Human Brain Atlas; **BR** = brain reserve; **DBM** = deformation-based morphometry; **FDR** = false discovery rate; **GO** = gene ontology; **H&Y** = Hoehn and Yahr; **LME** = linear mixed effects; **MDS-UPDRS** = Movement Disorder Society–sponsored revision of the Unified Parkinson's Disease Rating Scale; **NC** = normal control; **PAP** = progression-associated pattern; **PC** = principal component; **PD** = Parkinsons disease; **PIGD** = postural instability and gait disorder; **PPMI** = Parkinson's Progression Markers Initiative; **SNc** = substantia nigra pars compacta.


### Discussion

Patients with PD with greater brain resources (that is, higher deformation-based morphometry values) had greater compensatory capacity, which was associated with slower rates of clinical progression. This knowledge could be used to stratify and monitor patients for clinical trials.


Heterogeneity in the rates of progression of Parkinson disease (PD) is well recognized.[1-3] Identifying markers related to progression can lead to a better understanding of underlying mechanisms, prediction of disease prognosis, and, eventually, identification of modifiable risk factors that may delay the progression of PD. To date, many attempts have been made to identify markers of prognosis, including age,[1,2,4] baseline clinical scores,[2,5-7] CSF and blood biomarkers,[8] gene sequence variation,[2,5,9-11] free water in the posterior substantia nigra,[12] white matter,[13,14] functional connectomics,[15] and atrophy patterns.[3] However, the prognostic value of structural measurements of brain reserve remains elusive. Nevertheless, they have been validated as prognostic biomarkers in other neurodegenerative diseases, such as Alzheimer disease.[16-18]

The substantia nigra pars compacta (SNc) is a major site of neurodegeneration in PD.[19] However, motor features appear only when approximately 50% of dopaminergic neurons have been lost in SNc.[20,21] This delayed appearance of clinical signs is due to the existence of compensatory mechanisms, which are defined as the changes in the neural circuits that mitigate the effects of the loss of damaged neurons to maintain function or behavior.[22,23] Furthermore, clinical scores correlate with the loss of subcortical volumes[24,25] and dopaminergic dysfunction,[26] demonstrating that the number and size of neurons in subcortex are significantly associated with the clinical severity of patients. A recent study by our team found that among 2 biotypes of PD, 1 biotype with smaller subcortical volume has faster progression in several clinical domains.[27] Collectively, the above evidence suggests that neural resources (i.e., the number of available neurons, neuronal integrity, and synaptic density) may exert a protective effect on behavioral performance in PD. These neural resources are often referred to as brain reserve (BR), which is typically operationalized by brain volume in human neuroimaging studies.[28]

Herein, we test the hypothesis that patients with PD with greater BR capacity can tolerate a greater extent of brain damage and have lower rates of clinical progression, by examining associations between baseline deformation-based morphometry (DBM) values and the annual rate of change in clinical scores. In addition, we integrated multiple modalities to provide a possible mechanistic basis for structural measurements of brain reserve in PD.

## Methods

### Participants

Participants in this study were recruited from 2 cohorts: the Parkinson's Progression Markers Initiative (PPMI; http://www.ppmi-info.org)[29] and Huashan Hospital, Fudan University. The PPMI is a prospective, longitudinal, observational multicenter study that aims to verify biomarkers of PD.[29] The inclusion criteria for patients with PD in the PPMI cohort were the following: (1) diagnosed with PD less than 2 years, (2) baseline Hoehn and Yahr stage I to II, (3) dopaminergic deficit on imaging, and (4) never treated with dopamine replacement therapy.[29] Study visits for participants from the PPMI occurred at baseline, every 3 months during the first year, and every 6 months during the subsequent 4 years (eTables 1 and 2, links.lww.com/WNL/C117). Only patients with baseline MRI data and at least 2 years of follow-up were included in our analysis. Therefore, 346 patients with PD and 171 normal controls were included from the PPMI cohort (Table 1). The data used in this study were obtained from the PPMI website on April 2021.

The Huashan Hospital cohort consisted of 23 normal controls, 43 patients with PD who underwent MRI and clinical follow-up, and 97 patients with PD who underwent PET scanning (eTables 3 and 4, links.lww.com/WNL/C117). Patients with PD were diagnosed by movement disorder specialists according to the UK Parkinson's Disease Society Brain Bank criteria,[30] and they were followed up for at least 2 years.

### Standard Protocol Approvals, Registrations, and Patient Consents

The study was approved by the institutional review board at each PPMI site and the Research Ethics Committee of Huashan Hospital, Shanghai, China. Written informed consent was obtained from all patients participating in the study.

## T1-Weighted MRI Processing

The T1-weighted MRIs were preprocessed with the Computational Anatomy Toolbox (CAT12).[31] Raw MRIs of lower quality (CAT image quality rating <75%) were excluded. We used DBM values as a measure of BR. DBM is based on the application of nonlinear registration procedures to spatially normalize each MRI to the standard brain template (Montreal Neurological Institute ICBM-152). The nonlinear transformations were used to calculate deformation at each voxel to yield local volume changes, which were quantified by a mathematical property of these deformations (the Jacobian determinant).[32] By performing this calculation at each voxel, a map of local volume changes between each MRI and the MNI152-2009c template were obtained. Please see eMethods for more details (links.lww.com/WNL/C117).

## Baseline and Follow-up Clinical Assessments

Demographic characteristics, including age, sex, race, duration of symptoms, and education level, were recorded at baseline (Table 1). The following assessments were used in this study: Movement Disorder Society–sponsored revision of the Unified Parkinson's Disease Rating Scale (MDS-UPDRS)—Part I (nonmotor experiences of daily living), Part II (motor experiences of daily living), Part III (motor examination), total MDS-UPDRS scores, postural instability–gait difficulty (PIGD) scores, and Schwab & England ADL (activities of daily living) scale, which together capture major PD symptoms, including both motor and nonmotor symptoms. A previous study has found that the UPDRS Part II score and Part III score and the Schwab & England Independence Scale score can be used to measure disease progression in early PD.[33] To make the Schwab & England ADL have the same change direction as that of other scores, the Schwab & England ADL was calculated as one hundred (full marks) minus raw score. For patients with PD from the Huashan dataset, only the PIGD score and UPDRS Part III were recorded.

## Linear Mixed-Effects Models Examining Associations Between Baseline DBM Values and Clinical Progression

Using T1-weighted MRI data and longitudinal clinical data of patients with PD from the PPMI dataset[29,34] and Huashan dataset, we investigated the relationship between baseline DBM values and the annual rate of change in clinical scores using linear mixed-effects (LME) models. We used a separate model for each clinical score (i.e., MDS-UPDRS-I, MDS-UPDRS-II, MDS-UPDRS-III, MDS-UPDRS-III, PIGD score, and Schwab & England ADL) (Eq. (1)).

$$\begin{aligned}\text{Score} \sim 1 + \text{sex} + \text{age} + \text{race} + \text{education} + \text{time} \\ + \text{DBM values} + \text{study sites} + \text{DBM values} \times \text{time} \\ + (1 + \text{time}|\text{subj})\end{aligned} \quad (1)$$

All models were implemented in MATLAB 2018b using the *fitlme* function. In each model, we included sex, age, race, education, time (since symptoms), DBM values at baseline, study sites' effects, and interaction of DBM values and time as fixed effects. The participant slope and intercept were modeled as random effects. These LME models were performed voxel by voxel, and β-coefficients were computed (Figure 1A). For simplicity, hereafter, we will refer to the spatial patterns of β-coefficients as progression-associated patterns (PAP).

## Spatial Correlation Analysis With PET and Structural Changes

We used *t* values (case-control difference) of the PET data and T1-weighted MRI from PD and control groups to investigate their relationships with PAPs. PET images were scanned at Huashan Hospital. The preprocessing of PET data was performed as previously described (please see eMethods for more details, links.lww.com/WNL/C117).[26,35] The 2b-carbomethoxy-3b-(4-trimethylstannylphenyl) tropane ($^{11}$C-CFT) PET data provide an assessment of the spatial distribution of dysfunction in presynaptic dopaminergic binding, and $^{18}$F-fluorodeoxyglucose ($^{18}$F-FDG) PET provides a measure of metabolic abnormalities in PD at the system level. Therefore, we were able to test the associations between PAPs and *t* values of these PET markers yielded from comparison between patients with PD and healthy controls (Figure 1B). Before performing correlation analyses, we resampled PAPs (1.5 × 1.5 × 1.5 mm) to the same dimension of the PET images (2 × 2 × 2 mm) to make them share the same spatial resolution. Please see eMethods for more details.

## Transcriptomic Analysis

We integrated transcriptome data to provide a possible mechanistic basis for structural measurements of BR in PD. Transcriptional datasets with gene expression measurements in 6 postmortem adult (independent of the participants with PD) brains were acquired from the Allen Human Brain Atlas (AHBA).[36] We used the recently described rigorous preprocessing pipeline,[37] including probe-to-gene reannotation, intensity-based data filtering, probe selection by maximum coefficient of variation across samples, normalizing the gene expression data separately for each subject, and gene filtering by differential stability, finally resulting in 15,745 unique genes (see Arnatkevičiūtė et al., 2019, and eMethods, links.lww.com/WNL/C117).

Next, we investigated the correlation between the individual expression profiles of each of the 15,745 AHBA genes and PAPs. We used an online web tool, ToppGene Suite,[38,39] to perform the gene-set analysis with the top genes as input. Please see eMethods for more details (links.lww.com/WNL/C117).

## Statistical Analysis

Pearson correlations were performed between clinical scores at each time point and baseline subcortical DBM values to test whether the *R* values of DBM values and follow-up scores changed with time. The *t* test was used to determine the statistical significance of continuous variables. Before performing correlation analyses and the *t* test, confounding variables such as sex, age, years of education, race (categorized as White or other), and study sites' effects, were regressed out. The $\chi^2$ test was used to test the significance of categorical variables. The values were

**Table 1** Baseline Demographics and Clinical Characteristics of Participants With T1-MRI From 2 Datasets

| | Main cohort (PPMI dataset) | | Validation cohort (Huashan dataset) | |
|---|---|---|---|---|
| **Demography** | **Controls (n = 171)** | **PD (n = 346)** | **Controls (n = 23)** | **PD (n = 43)** |
| **Age at onset, y** | 60.5 (11.19) | 61.29 (10.03) | 60.78 (6.08) | 59.35 (7.32) |
| **Sex (male: female)** | 110:61 | 225:121 | 17:6 | 31:12 |
| **Education history, y** | 16.14 (2.92) | 15.61 (2.9) | — | — |
| **Symptom duration,[a] y** | — | 0.58 (0.57) | — | 1.78 (1.52) |
| **H&Y** | — | 1.55 (0.51) | — | 1.52 (0.67) |
| **UPDRS total score[b]** | 4.48 (4.5) | 31.89 (13.03) | — | — |
| **UPDRS Part I[b]** | 2.92 (3.04) | 5.55 (3.97) | — | — |
| **UPDRS Part II[b]** | 0.43 (0.98) | 5.81 (4.09) | — | — |
| **UPDRS Part III[b]** | 1.19 (2.26) | 20.55 (8.76) | — | 17.84 (9.20) |
| **PIGD[a,b]** | 0.02 (0.09) | 0.23 (0.23) | — | 0.33 (0.20) |
| **Schwab & England ADL** | — | 93.37 (5.74) | — | — |

Abbreviations: ADL = activities of daily living; H&Y = Hoehn and Yahr; PIGD = postural instability–gait difficulty; PD = Parkinson disease; PPMI = Parkinson's Progression Markers Initiative; UPDRS = Unified Parkinson's Disease Rating Scale
Values are presented as mean (SD).
[a] Differences between patients from the 2 PD cohorts, $p < 0.05$.
[b] Differences between normal controls and patients with PD in the PPMI dataset, $p < 0.05$.

reported as mean (SD) for each demographic and clinical variable. Missing data were not included in any analyses.

## Data Availability

Data used in the preparation of this article were obtained from the Parkinson's Progression Markers Initiative (PPMI) database (www.ppmi-info.org). For up-to-date information on the study, visit ppmi-info.org. Anonymized data from Huashan Hospital will be made available to research investigators on request to the corresponding author.

# Results

## Demographics and Clinical Variables

Patients with PD (n = 389) with T1-MRI and follow-up clinical assessments from 2 cohorts (n = 346, age 61.3 ± 10.03, 35% female, PPMI dataset; n = 43, age 59.4 ± 7.3, 38.7% female, Huashan dataset) were included. At baseline, there were no significant demographic differences between the normal controls and the patients with PD or between the PD patients in the PPMI dataset and the Huashan dataset (Table 1). The duration of symptoms tended to be longer in the Huashan dataset than in the PPMI dataset ($p < 0.05$). No significant differences in UPDRS-III were observed in patients with PD between 2 datasets ($p > 0.05$). However, the PIGD score was higher in the Huashan dataset than in the PPMI dataset ($p < 0.05$). Clinical and demographic data are summarized in Table 1 for both datasets.

## Correlations Between Baseline DBM Values and Motor Progression

To examine whether baseline DBM values correlated with clinical progression, LME models were performed including the bivariate interaction of the baseline DBM value and time for the clinical score as the dependent variable. Voxel-wise analysis by LME models revealed significant interaction of subcortical baseline DBM values and time for 4 clinical assessments (i.e., MDS-UPDRS Part II, total MDS-UPDRS scores, PIGD score, and Schwab & England ADL score) as the dependent variable, respectively ($p < 0.05$, false discovery rate [FDR] corrected; Figure 2, eTable 5, links.lww.com/WNL/C117). The interactions were evident in all subcortical regions but more marked in the putamen. Interactions of subcortical baseline DBM values and time on longitudinal change in MDS-UPDRS Part I, III did not survive after controlling for multiple comparisons using FDR. Therefore, results with a more liberal threshold ($p < 0.005$, uncorrected) are displayed in eFigure 1. At 1-year follow-up, 153 of the 346 patients with PD underwent T1-MRI scan of the PPMI (eTable 1). We found a significant interaction of subcortical DBM values at 1-year follow-up and time (clinical data over the following 4 years) for the PIGD score as the dependent variable ($p < 0.05$, FDR corrected; eFigure 2).

To validate our findings, we repeated LME models analyses in a separate dataset from Huashan Hospital with MRI data accessible at baseline and follow-up clinical scores (n = 43, Table 1). We found significant interactions between subcortical DBM values at baseline and time on longitudinal change in UPDRS-III and PIGD scores ($p < 0.05$, uncorrected; eFigure 3, links.lww.com/WNL/C117). Furthermore, PAPs from the 2 datasets were significantly correlated ($p < 0.05$, uncorrected; Figure 3, eFigures 4–6). Together, these results suggest that the patients had lower DBM values of subcortical regions with faster deterioration of these scores. Voxels with significant

**Figure 1** Overview of the Study Methodology

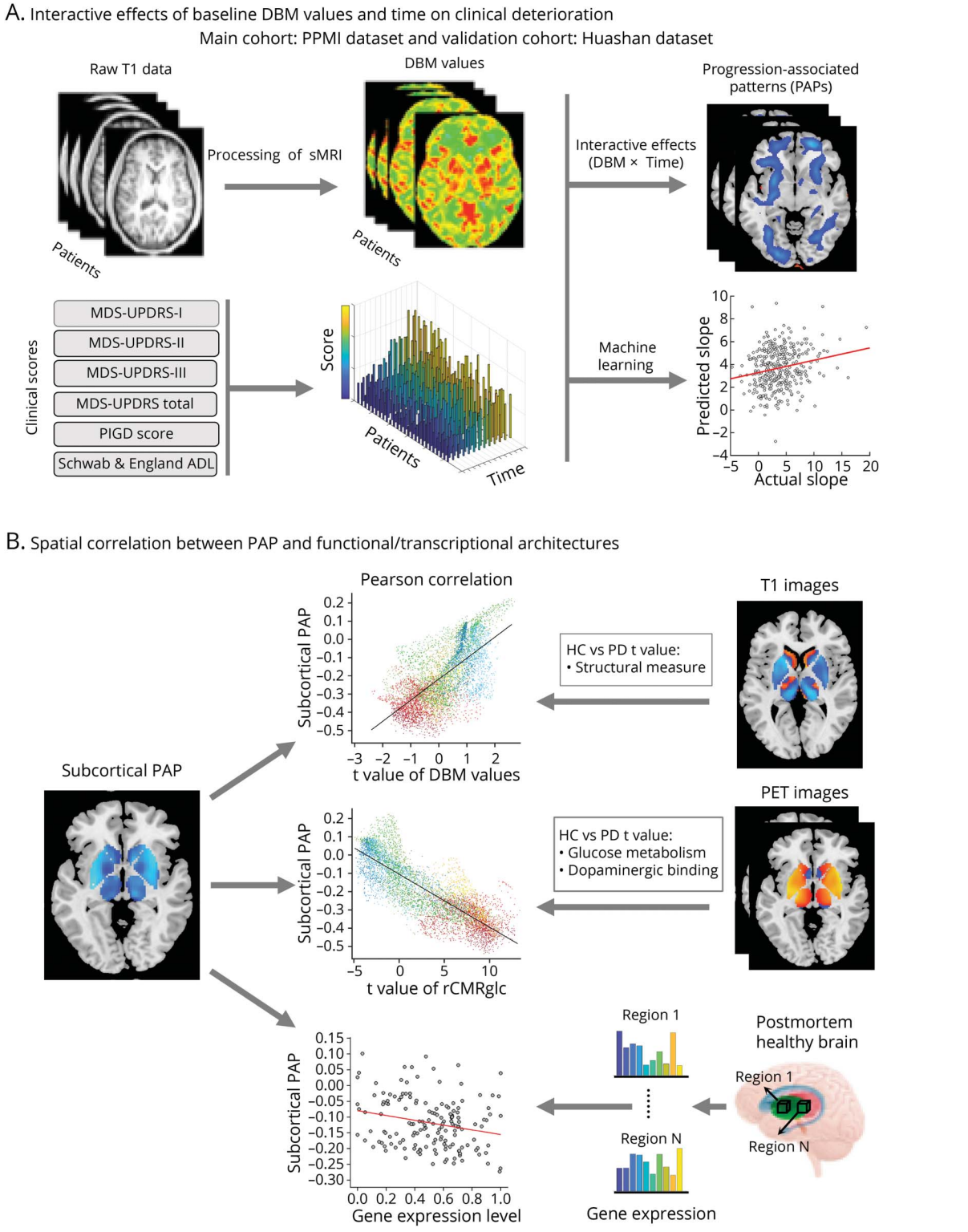


(A) LME models examining the interactive effects of baseline DBM values and time on clinical deterioration. T1-weighted MRI data and clinical data of follow-up were obtained from the PPMI and Huashan dataset. PAPs were obtained as β-coefficients by performing voxel-wise LME models analyses. (B) These PAPs were investigated using complementary analyses of neuroimaging data and transcriptomic data. Because voxels with significantly interactive effects with time on clinical deterioration were primarily located in subcortical regions, we focused on the PAPs of the subcortical regions. First row: case-control differences in subcortical DBM values in the 2 cohorts. T1-weighted MRI data were obtained from both the PPMI and Huashan dataset. Second row: case-control differences in PET. In this dual-tracer PET study, dopaminergic binding ($^{11}$C-CFT) and glucose metabolism ($^{18}$F-FDG) data were obtained at Huashan dataset. Third row: gene expression data in the subcortical regions were extracted. The obtained subcortical gene expression patterns were correlated with PAPs. $^{11}$C-CFT = 2b-carbomethoxy-3b-(4-trimethylstannylphenyl) tropane; $^{18}$F-FDG = $^{18}$F-fluorodeoxyglucose; DBM = deformation-based morphometry; HC = healthy control; LME = linear mixed effects; PAP = progression-associated pattern; PD = Parkinson disease.

**Figure 2** Voxels With Significant Interactive Effects on Clinical Deterioration

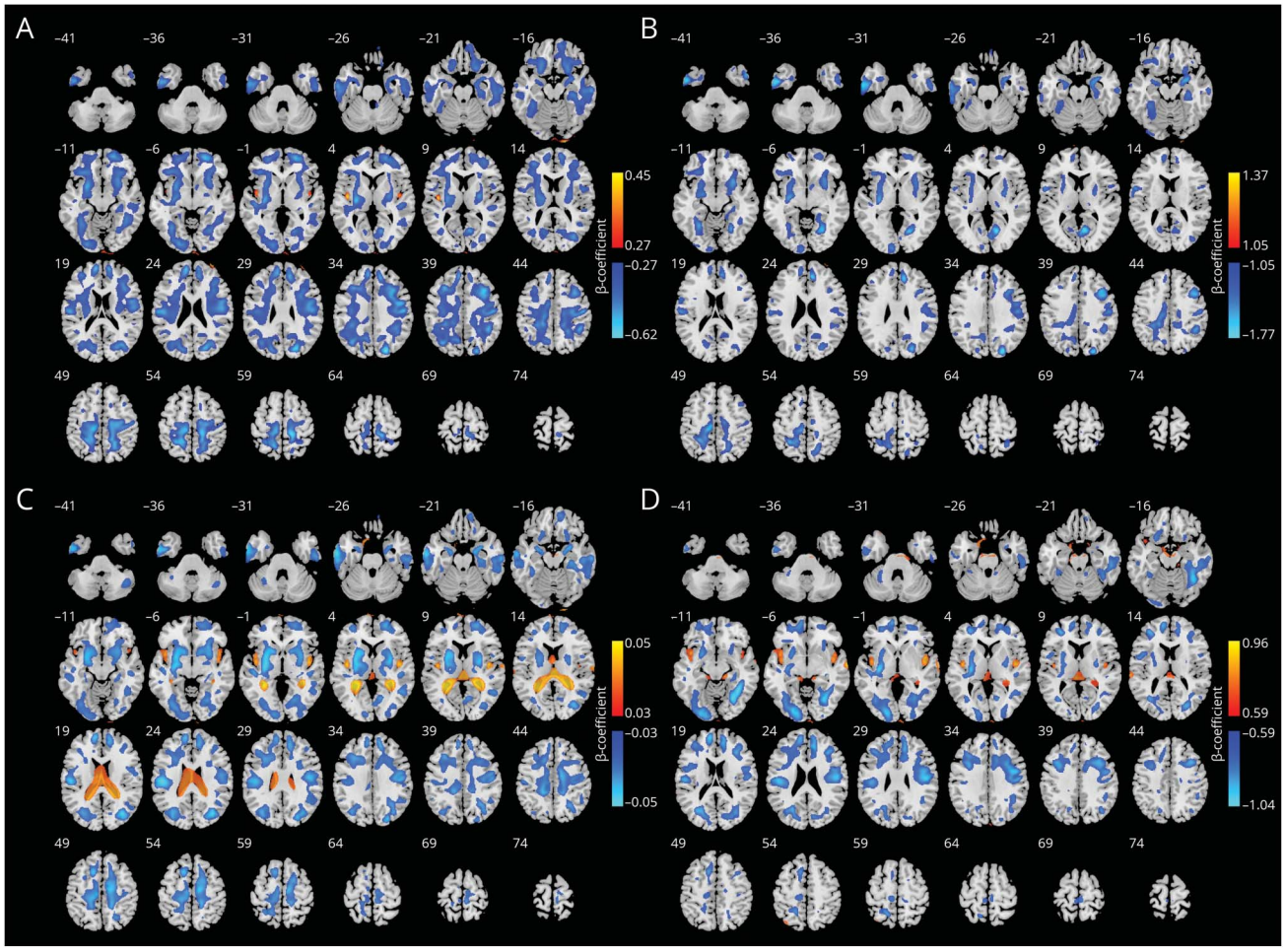


Significant β-coefficients ($p < 0.05$, FDR corrected) for the interactive effects between baseline DBM values and time on deterioration of MDS-UPDRS Part II (A), MDS-UPDRS total scores (B), PIGD score (C), and Schwab & England ADL score (D). Warm colors indicate positive β-coefficients; cold colors indicate negative β coefficients. ADL = activities of daily living; DBM = deformation-based morphometry; FDR = false discovery rate; MDS-UPDRS = Movement Disorder Society–sponsored revision of the Unified Parkinson's Disease Rating Scale; PIGD = postural instability–gait difficulty.

interactive effects on clinical deterioration were primarily located in subcortical regions, which are commonly studied and have received attention in the context of PD studies[3,26,27,40,41]; therefore, we focused on subcortical regions (i.e., the putamen, caudate, pallidum, and thalamus) in this study.

For visualization purposes, patients with PD were divided into 3 groups based on the regional DBM values of subcortical regions. The 3 groups created using regional DBM values of putamen were strongly differentiated (eFigure 7, links.lww.com/WNL/C117). Specifically, individuals with low putamen DBM values had the steepest slope for all 6 clinical scores, followed by medium putamen DBM values and then followed by individuals with high putamen DBM values. Individuals with low regional DBM values of caudate, pallidum, and thalamus DBM values had the steepest slope for 3 clinical scores (i.e., MDS-UPDRS Part II, III, and total MDS-UPDRS scores).

## Correlations Between Baseline Subcortical DBM Values and Follow-up Clinical Scores

To further support the relationship between baseline DBM values and motor progression, we also tested whether the *r* values of DBM values and follow-up scores changed with time. To this end, we correlated DBM values with clinical scores at each time point and then performed a secondary correlation of these *r* values over time at the voxel level. Regional *r* values were extracted by averaging the secondary voxel *r* values within each subcortical region defined by the AAL2 atlas.[42] Then, we performed correlation analyses between subcortical regional *r* values and time from baseline. We found that regional *r* values of both left and right caudate with MDS-UPDRS Part II scores were significantly correlated with time, meaning that *r* values were lower closer to PD diagnosis and increased with time (eFigure 8, links.lww.com/WNL/C117; $p < 0.05$, uncorrected). Similar results were found between these 2 measures with the caudate (both left and right) and MDS-UPDRS-total and the

**Figure 3** Validation of PAPs From the PPMI Dataset Using Data From the Huashan Dataset

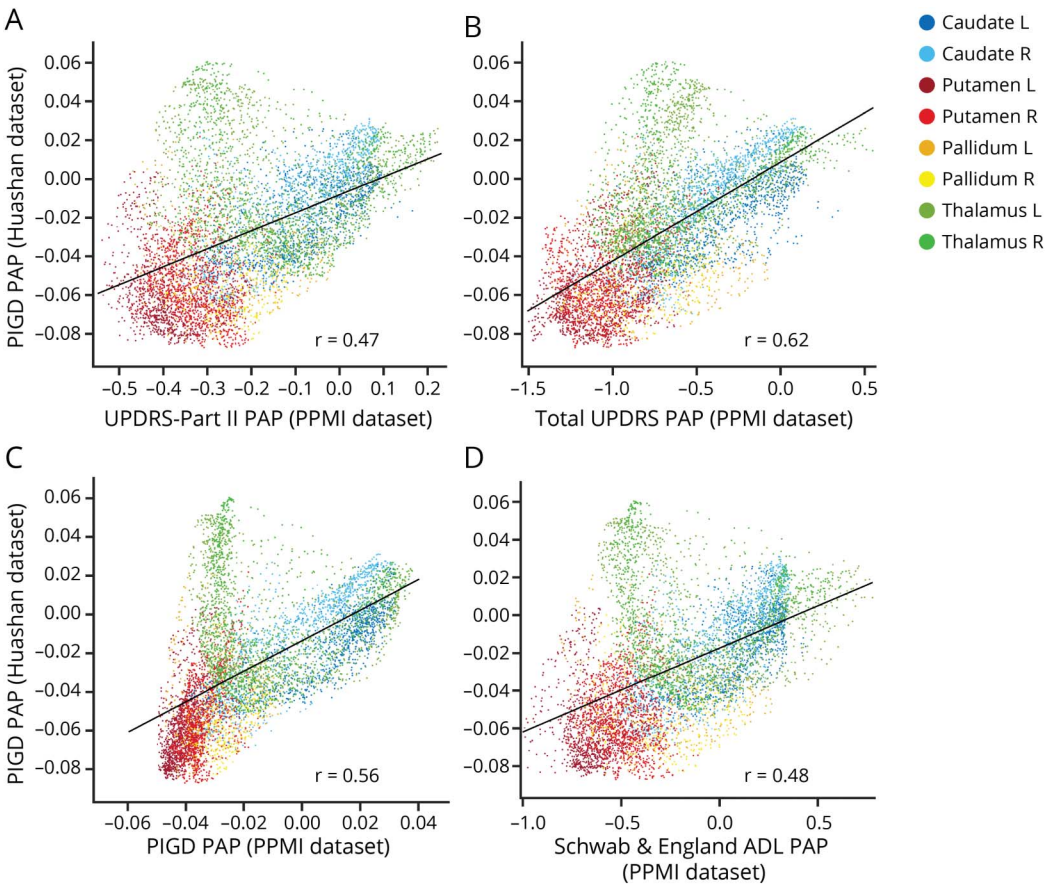


Correlations between PIGD PAP from Huashan dataset with UPDRS Part II PAP (A), MDS-UPDRS total score PAP (B), PIGD PAP (C), and Schwab & England ADL score PAP (D) from the PPMI dataset. ADL = activities of daily living; DBM = deformation-based morphometry; MDS-UPDRS = Movement Disorder Society–sponsored revision of the Unified Parkinson's Disease Rating Scale; PAP = progression-associated pattern; PIGD = postural instability–gait difficulty; PPMI = Parkinson's Progression Markers Initiative.

left putamen and Schwab & England ADL scores. These results suggested that patients with PD with lower subcortical DBM values at baseline tended to have higher clinical scores at the follow-up visit.

## Prediction of the Individual Motor Progression

To test whether baseline DBM values could predict individual progression of PD, we trained predictive models with fitted rates of progression as a dependent variable. The annual rate of change in the clinical score was estimated using LME models for each individual (see eMethods for more details, links.lww.com/WNL/C117). Principal component (PC) analysis was applied to characterize low-dimensional subcortical DBM values. The first PC, which explained 46.15% of variance in subcortical DBM values across all voxels, was negatively correlated with progression based on 5 clinical scores, including MDS-UPDRS Part I, II, and total scores, PIGD scores, and Schwab & England ADL scores ($p < 0.05$, FDR corrected; eFigure 9). Then, tenfold cross validation was used to estimate the prospective predictive performance for trained models using internal PPMI samples, with $r$ values of Pearson correlation (predicted vs observed progression rates). The results showed significant predictions of clinical progression (progression based on MDS-UPDRS Part II: $r = 0.21$; progression based on total MDS-UPDRS scores: $r = 0.21$; progression based on PIGD scores: $r = 0.24$; progression based on Schwab & England ADL scores: $r = 0.23$; all $p < 0.05$, FDR corrected; eFigure 10). These results suggested that subcortical DBM values capture meaningful neurobiological features that support distinct rates of motor progression.

## Correlations Between PAPs and Dopaminergic Binding, Metabolic, and Structural Changes

PD is associated with dopaminergic dysfunction, abnormal metabolism, and subcortical atrophy.[26,36,40,43] We thus tested whether the spatial distribution of PAPs would recapitulate the distribution of changes in dopaminergic binding and metabolic and structural measures. This might then reinforce that the brain areas where higher DBM values afford protection against clinical progression are those implicated in dopaminergic binding, metabolic and structural change. Using dual-tracer PET data combined with assessments of dopaminergic binding ($^{11}$C-CFT) and glucose metabolism ($^{18}$F-FDG) in patients with PD and normal controls from the Huashan

**Figure 4** Spatial Association Between PAPs and Case-Control Differences in DAT Binding, $^{18}$F-FDG Metabolism, and DBM Values in Subcortical Regions

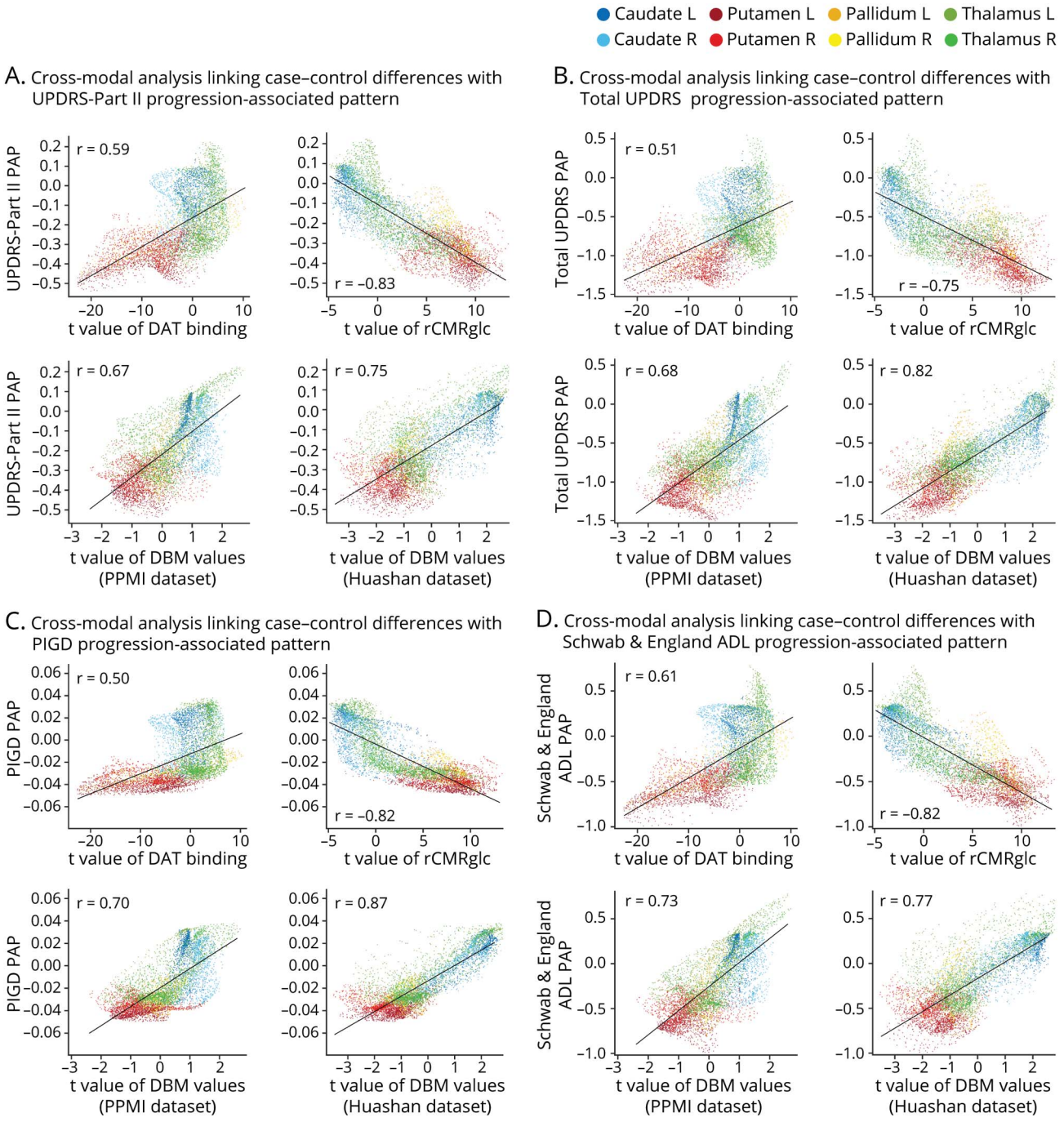


The *t* statistic map indexes voxel-wise differences in DAT binding, $^{18}$F-FDG metabolism, and DBM values between the patients with PD and healthy participants (that is, a higher absolute *t* statistic value corresponds to a more severe abnormality in this voxel). DAT binding and $^{18}$F-FDG metabolism were obtained from the Huashan dataset. DBM values were obtained from both the PPMI dataset and Huashan dataset. (A) Results of spatial correlation analyses between MDS-UPDRS Part II PAP (A), MDS-UPDRS total score PAP (B), PIGD PAP (C), and Schwab & England ADL PAP (D) with case-control differences in DAT binding, $^{18}$F-FDG metabolism, and DBM values. $^{11}$C-CFT = 2b-carbomethoxy-3b-(4-trimethylstannylphenyl) tropane; $^{18}$F-FDG = $^{18}$F-fluorodeoxyglucose; ADL = activities of daily living; DAT = dopamine transporter; DBM = deformation-based morphometry; MDS-UPDRS = Movement Disorder Society–sponsored revision of the Unified Parkinson's Disease Rating Scale; PAP = progression-associated pattern; PIGD = postural instability–gait difficulty; PPMI = Parkinson's Progression Markers Initiative; rCMRglc = regional cerebral metabolic rate of glucose.

dataset, the spatial distribution of *t* values in subcortical regions was obtained. PAPs across the spatial extent of subcortical regions were positively correlated with the *t* values of $^{11}$C-CFT and negatively correlated with the *t* values of $^{18}$F-FDG (Figure 4, eFigure 11, links.lww.com/WNL/C117). The positive correlations with the *t* values of $^{11}$C-CFT suggested that voxels that lose more dopaminergic innervation could contribute more to protecting against

**Figure 5** Gene Expression Patterns Underlie PAPs

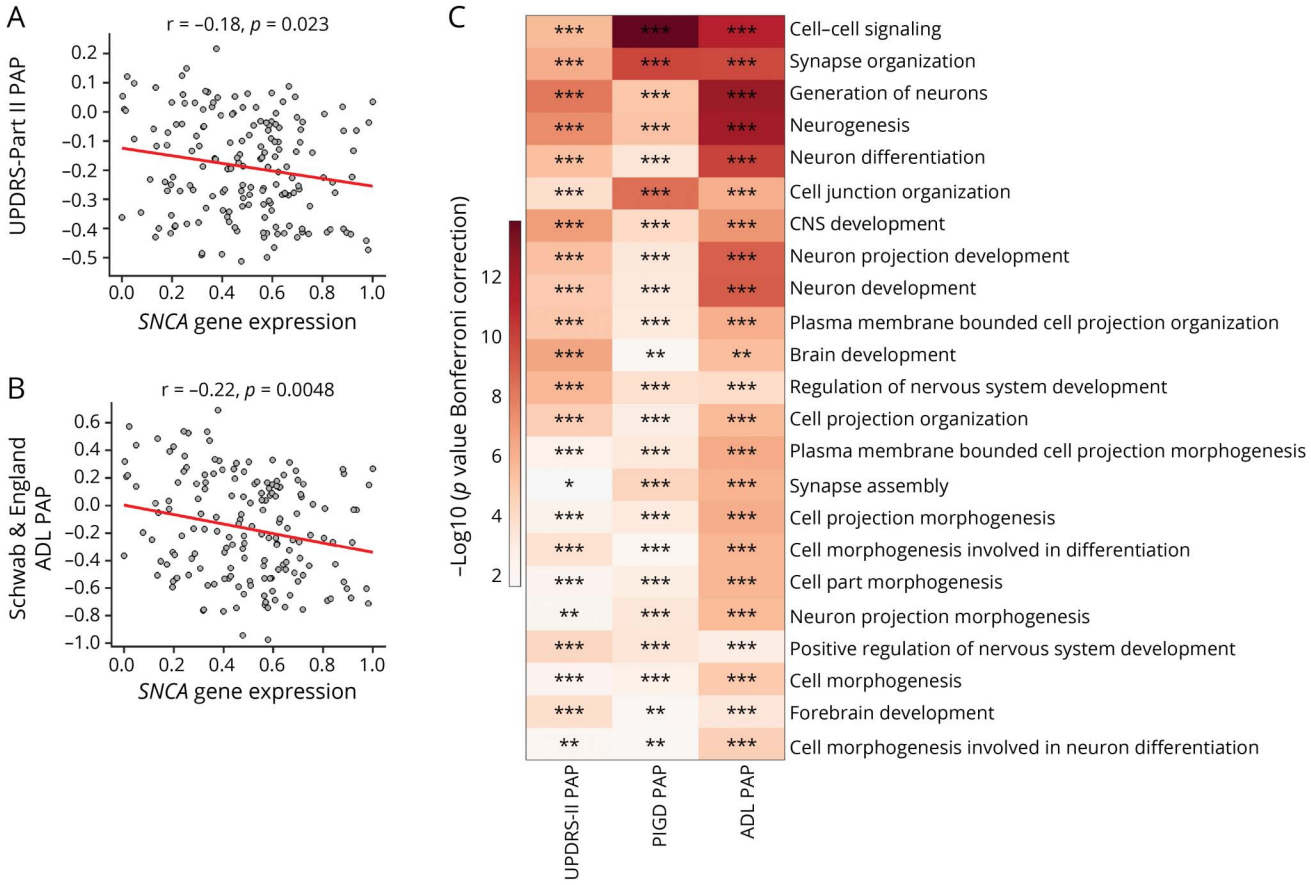


(A and B) Scatterplot of MDS-UPDRS Part II PAP (A), Schwab & England ADL PAP (B) and *SNCA* gene expression measures. Pearson correlation coefficients and *p* values are shown above the plot. (C) Enrichment analysis of the positively correlated genes, involved in different biological processes, for each PAP. The *p* values are Bonferroni corrected for multiple comparisons. **p* < 0.05, ***p* < 0.01, and ****p* < 0.005. ADL = activities of daily living; MDS-UPDRS = Movement Disorder Society–sponsored revision of the Unified Parkinson's Disease Rating Scale; PAP = progression-associated pattern.

clinical deterioration. The negative correlation with the $^{18}$F-FDG *t* value map suggested that voxels with elevated metabolic activity might be compensating more to protect against PD pathology.[44,45] In addition, there were strong positive correlations between PAPs and the *t* values of DBM values in each of the 2 cohorts, suggesting that voxels with greater atrophy could contribute more to protect against clinical deterioration. These correlations still existed within distinct subcortical regions (eFigures 12–15). These correlations of PAPs and the *t* value map were replicated using validation data from Huashan Hospital, with details provided in eFigure 16.

## Correlations Between PAPs and Gene Expression Patterns

We then investigated whether the spatial distribution of PAPs could recapitulate the expression of some PD risk genes in subcortical regions. The set of putative PD risk factor genes from the GWAS meta-analysis[46] was mapped to the standard brain template. Among PD risk genes correlated with PAPs, there were both positive and negative correlations. A negative correlation indicated that these PD risk factor genes were highly expressed in sites related to clinical progression and vice versa. Of interest, α-synuclein gene (*SNCA*) expression patterns negatively correlated with PAPs (Figure 5, eFigure 17, links.lww.com/WNL/C117). The expression of some other genes is negatively correlated with PAPs, including *KLHL7*, *DDRGK*, and *COQ7* ($p < 0.05$, FDR corrected; eFigure 18). Genes had expression patterns that were positively correlated with PAPs, including *TOX3*, *ZNF646*, *CAMK2D*, and *TMEM163* ($p < 0.05$, FDR corrected; eFigure 18).

We continued by examining the correlations between PAPs and each of the 15,745 individual AHBA genes and selecting significantly correlated genes ($p < 0.05$, FDR correction). See eTables 6 and 7 (links.lww.com/WNL/C117) for a complete list of genes. To obtain clues about possible biological functions of the genes with expression levels related to PAPs, we subjected these genes to gene ontology (GO) enrichment analysis. The positively (MDS-UPDRS II PAP, PIGD PAP, and Schwab & England ADL PAP) and

negatively (MDS-UPDRS III PAP) correlated genes were both enriched in the biological processes of neurogenesis, neuron differentiation, generation of neurons, and cell part morphogenesis (Figure 5C, eTables 8 and 9). The negatively correlated genes were enriched in the biological process glutamate secretion. Glutamatergic neurons are rich in basal ganglia and involved in both motor symptoms and nonmotor symptoms in patients with PD.[47] No biological process was enriched for genes that negatively correlated MDS-UPDRS II PAP, PIGD PAP, and Schwab & England ADL PAP.

## Discussion

In this study, we found that (1) patients with low subcortical DBM values are associated with faster progression of motor symptoms across the 2 datasets. Despite the relatively small sample size of the validation dataset and some sample bias (i.e., baseline clinical measures, clinical follow-up, MRI acquisitions, and participant ethnicity), the cross-validations support a general trend between brain reserve and PD motor progression. (2) Progression-associated patterns were spatially associated with dopaminergic dysregulation and metabolic and structural changes in PD and the expression of the α-synuclein gene. Overall, we found that structural measurements of brain reserve are associated with motor progression in PD.

Under the assumption that progressive loss of dopaminergic neurons causes clinical symptoms,[21] higher subcortical DBM values may reflect greater brain resources acting as a buffer that enables the brain to better tolerate emerging neuropathology. These interactions were more marked in the putamen, which is consistent with previous studies that showed that the functional and structural connectivity of the basal ganglia predicts clinical progression in patients with PD.[14,15] PAPs recapitulate the spatial distribution of case-control differences in dopaminergic and structural measures, suggesting that voxels that show more abnormality in PD are also more important in compensating against clinical deterioration. The negative correlation between the PAPs and metabolic changes may reflect protective or compensatory metabolic activities in response to PD pathology.[22,26,44,48] Therefore, patients with PD with higher DBM values in subcortical regions showed better compensatory capacity, resulting in slower rates of clinical progression, than PD patients with lower DBM values in subcortical regions. Thus, our findings provide supporting evidence for the theory of a compensatory role of BR.[22,23] This is in line with a series of articles indicating that BR acts as a resilience factor against clinical deterioration in the presence of neuropathology[16,18,49] and that compensatory mechanisms decline as PD progresses.[48]

GO analysis identified biological processes of neurogenesis, neuron differentiation, generation of neurons, and cell part morphogenesis, indicating that these processes may involve in a compensatory role in PD.[50] It is thus possible that new neurons may enable compensation in PD.[50] This process allows the brain to reorganize its structure and brain functional networks to actively cope with neuropathology.[23,50] Therefore, our finding that baseline structural measurements of BR are associated with motor progression in PD may help maximize the information gleamed from trials of potential disease-modifying therapies, such as stem cell implants.[50,51] This arises because brain reserve measures in the form of baseline DBM values may provide a means of identifying patients who are more likely to deteriorate rapidly. Enrichment of disease-modifying trials with such patients may lead to greater effect sizes and shorter studies.

Some limitations of this study should be considered. First, for the longitudinal analyses, we used clinical scores with 5-year follow-up duration that were used. Five years is a relatively long time for a longitudinal study but was not enough to cover the full course of PD. It is possible that future longitudinal studies with longer follow-up periods could further investigate these associations. Second, these 4 clinical scores (MDS-UPDRS Part II, total MDS-UPDRS scores, PIGD score, and Schwab & England ADL score) predominantly capture motor symptoms, and future research should be undertaken to incorporate additional nonmotor symptoms of PD, such as psychiatric[7,20] and cognitive symptoms,[25,52] to investigate the relationship between BR and nonmotor progression in a larger dataset. Third, the PPMI recruited participants who were younger than the general PD population, and as such, the PPMI dataset cannot be considered to be representative of the natural history of PD progression.[29,34] Fourth, the interpretation of our cross-validation is constrained by some sample bias including the small sample size, baseline clinical measures, clinical follow-up, MRI acquisitions, and participant ethnicity. Theses sample bias may limit the generalizability of our findings. Replication of findings in future studies with shorter baseline duration, longer follow-up periods, more comprehensive clinical assessments, and ethnically more diverse sample is required. Fifth, the first PC of subcortical DBM values explained only a relatively small proportion of the total variance in fitted slopes of change in motor symptoms, suggesting the BR may be only factor of many determining clinical progression.[1-15] Finally, the whole-brain data on normal brain tissue expression of the genome were measured in 6 postmortem donors (mean age = 43 years) and not in age-matched patients with PD. Therefore, the expression data are limited to examining relationships between subcortical patterns of gene expression and the association patterns between clinical progression and structural measures.

Overall, we found that structural measurements of BR affect the clinical progression of motor symptoms in patients with PD. Although further validation and independent tests on data from larger populations and longer follow-up time will be required to provide more definitive evidence for the robustness and generalizability of the effects, our results on generalizability across 2 separate datasets provide a meaningful step toward a

neuroimaging biomarker that can quantitatively assess motor progression in PD.

## Study Funding

J. Feng is supported by National Key R&D Program of China (No. 2018YFC1312904), National Key R&D Program of China (No. 2019YFA0709502), Shanghai Municipal Science and Technology Major Project (No. 2018SHZDZX01), ZJ Lab, Shanghai Center for Brain Science and Brain-Inspired Technology, and the 111 Project (No. B18015). W. Cheng is supported by grants from the National Natural Sciences Foundation of China (No.82071997) and the Shanghai Rising Star Program (No. 21QA1408700). Peter Brown is supported by the Medical Research Council (MC_UU_12024/1). C. Zuo is supported by the National Natural Science Foundation of China (No. 82021002, 81971641 and 81671239), research project of Shanghai Health Commission(2020YJZX0111); Clinical Research Plan of SHDC (SHDC2020CR1038B); Science and Technology Innovation 2030 Major Projects (2022ZD0211600). P. Wu is supported by the National Natural Science Foundation of China (No. 81771483) and Shanghai Municipal Health Commission (Youth Medical Talents - Medical Imaging Practitioner Program, No. SHWRS(2020)_087). PPMI – a public-private partnership – is funded by the Michael J. Fox Foundation for Parkinson's Research funding partners 4D Pharma, Abbvie, Acurex Therapeutics, Allergan, Amathus Therapeutics, ASAP, Avid Radiopharmaceuticals, Bial Biotech, Biogen, BioLegend, Bristol-Myers Squibb, Calico, Celgene, Dacapo Brain Science, Denali, The Edmond J. Safra Foundaiton, GE Healthcare, Genentech, GlaxoSmithKline, Golub Capital, Handl Therapeutics, Insitro, Janssen Neuroscience, Lilly, Lundbeck, Merck, Meso Scale Discovery, Neurocrine Biosciences, Pfizer, Piramal, Prevail, Roche, Sanofi Genzyme, Servier, Takeda, Teva, UCB, Verily, and Voyager Therapeutics.

## Disclosure

The authors report no relevant disclosures. Go to Neurology.org/N for full disclosures.

## Publication History

Received by *Neurology* October 26, 2021. Accepted in final form April 19, 2022. Submitted and externally peer reviewed. The handling editor was Peter Hedera, MD, PhD.

## Appendix Authors

| Name | Location | Contribution |
|---|---|---|
| **Linbo Wang, PhD** | Institute of Science and Technology for Brain-inspired Intelligence, Fudan University; Key Laboratory of Computational Neuroscience and Brain-Inspired Intelligence (Fudan University), Ministry of Education, Shanghai, China | Drafting/revision of the manuscript for content, including medical writing for content; major role in the acquisition of data; study concept or design; and analysis or interpretation of data |
| **Ping Wu, MD** | PET Center, Huashan Hospital, Fudan University, Shanghai, China | Drafting/revision of the manuscript for content, including medical writing for content; major role in the acquisition of data; and analysis or interpretation of data |
| **Peter Brown, MD** | Medical Research Council Brain Network Dynamics Unit at the University of Oxford; Nuffield Department of Clinical Neurosciences, John Radcliffe Hospital, University of Oxford, United Kingdom | Drafting/revision of the manuscript for content, including medical writing for content, and analysis or interpretation of data |
| **Wei Zhang, MSc** | Institute of Science and Technology for Brain-inspired Intelligence, Fudan University; Key Laboratory of Computational Neuroscience and Brain-Inspired Intelligence (Fudan University), Ministry of Education, Shanghai, China | Analysis or interpretation of data |
| **Fengtao Liu, MD** | Department of Neurology, Huashan Hospital North, Fudan University, Shanghai, China | Drafting/revision of the manuscript for content, including medical writing for content, and major role in the acquisition of data |
| **Yan Han, MD** | Department of Neurology, Yueyang Hospital of Integrated Traditional Chinese and Western Medicine, Shanghai University of Traditional Chinese Medicine, China | Drafting/revision of the manuscript for content, including medical writing for content |
| **Chuan-Tao Zuo, MD** | PET Center, Huashan Hospital, Department of Neurology, Huashan Hospital North, and Human Phenome Institute, Fudan University, Shanghai, China | Drafting/revision of the manuscript for content, including medical writing for content; major role in the acquisition of data; and analysis or interpretation of data |
| **Wei Cheng, PhD** | Institute of Science and Technology for Brain-inspired Intelligence, Fudan University; Key Laboratory of Computational Neuroscience and Brain-Inspired Intelligence (Fudan University), Ministry of Education; Zhangjiang Fudan International Innovation Center, Shanghai, China; Department of Computer Science, University of Warwick, Coventry, United Kingdom; Fudan ISTBI—ZJNU Algorithm Centre for Brain-inspired Intelligence, Zhejiang Normal University, Jinhua, China | Drafting/revision of the manuscript for content, including medical writing for content; major role in the acquisition of data; study concept or design; and analysis or interpretation of data |

Continued

## Appendix *(continued)*

| Name | Location | Contribution |
|---|---|---|
| **Jianfeng Feng, PhD** | Institute of Science and Technology for Brain-inspired Intelligence, Fudan University; Key Laboratory of Computational Neuroscience and Brain-Inspired Intelligence (Fudan University), Ministry of Education; Zhangjiang Fudan International Innovation Center, Shanghai, China; Department of Computer Science, University of Warwick, Coventry, United Kingdom; Fudan ISTBI—ZJNU Algorithm Centre for Brain-inspired Intelligence, Zhejiang Normal University, Jinhua, China | Drafting/revision of the manuscript for content, including medical writing for content; study concept or design; and analysis or interpretation of data |

## References


1. Velseboer DC, Broeders M, Post B, et al. Prognostic factors of motor impairment, disability, and quality of life in newly diagnosed PD. *Neurology*. 2013;80(7):627-633.
2. Latourelle JC, Beste MT, Hadzi TC, et al. Large-scale identification of clinical and genetic predictors of motor progression in patients with newly diagnosed Parkinson's disease: a longitudinal cohort study and validation. *Lancet Neurol*. 2017;16(11):908-916.
3. Zeighami Y, Fereshtehnejad SM, Dadar M, Collins DL, Postuma RB, Dagher A. Assessment of a prognostic MRI biomarker in early de novo Parkinson's disease. *Neuroimage Clin*. 2019;24:101986.
4. Pagano G, Ferrara N, Brooks DJ, Pavese N. Age at onset and Parkinson disease phenotype. *Neurology*. 2016;86(15):1400-1407.
5. Liu G, Locascio JJ, Corvol JC, et al. Prediction of cognition in Parkinson's disease with a clinical–genetic score: a longitudinal analysis of nine cohorts. *Lancet Neurol*. 2017;16(8):620-629.
6. Tsiouris KM, Konitsiotis S, Koutsouris DD, Fotiadis DI. Prognostic factors of Rapid symptoms progression in patients with newly diagnosed Parkinson's disease. *Artif Intell Med*. 2020;103:101807.
7. Barrett MJ, Blair JC, Sperling SA, Smolkin ME, Druzgal TJ. Baseline symptoms and basal forebrain volume predict future psychosis in early Parkinson disease. *Neurology*. 2018;90(18):e1618-e1626.
8. Parnetti L, Gaetani L, Eusebi P, et al. CSF and blood biomarkers for Parkinson's disease. *Lancet Neurol*. 2019;18(6):573-586.
9. Iwaki H, Blauwendraat C, Leonard HL, et al. Genetic risk of Parkinson disease and progression: an analysis of 13 longitudinal cohorts. *Neurol Genet*. 2019;5(4):e348
10. Sun YM, Yu HL, Zhou XY, et al. Disease progression in patients with parkin-related Parkinson's disease in a longitudinal cohort. *Mov Disord*. 2021;36(2):442-448.
11. Tan MMX, Lawton MA, Jabbari E, et al. Genome-wide association studies of cognitive and motor progression in Parkinson's disease. *Mov Disord*. 2021;36(3):424-433.
12. Burciu RG, Ofori E, Archer DB, et al. Progression marker of Parkinson's disease: a 4-year multi-site imaging study. *Brain*. 2017;140(8):2183-2192.
13. Shu ZY, Cui SJ, Wu X, et al. Predicting the progression of Parkinson's disease using conventional MRI and machine learning: an application of radiomic biomarkers in whole-brain white matter. *Magn Reson Med*. 2021;85(3):1611-1624.
14. Abbasi N, Fereshtehnejad SM, Zeighami Y, Larcher KMH, Postuma RB, Dagher A. Predicting severity and prognosis in Parkinson's disease from brain microstructure and connectivity. *Neuroimage Clin*. 2020;25:102111.
15. De Micco R, Agosta F, Basaia S, et al. Functional connectomics and disease progression in drug-naïve Parkinson's disease patients. *Mov Disord*. 2021;36(7):1603-1616.
16. Guo LH, Alexopoulos P, Wagenpfeil S, Kurz A, Perneczky R. Brain size and the compensation of Alzheimer's disease symptoms: a longitudinal cohort study. *Alzheimers Dement*. 2013;9(5):580-586.
17. Van Loenhoud AC, Van Der Flier WM, Wink AM, et al. Cognitive reserve and clinical progression in Alzheimer disease: a paradoxical relationship. *Neurology*. 2019;93(4):E334-E346.
18. Groot C, Van Loenhoud AC, Barkhof F, et al. Differential effects of cognitive reserve and brain reserve on cognition in Alzheimer disease. *Neurology*. 2018;90(2):e149-e156.
19. Ehringer H, Hornykiewicz O. Distribution of noradrenaline and dopamine (3-hydroxytyramine) in the human brain and their behavior in diseases of the extrapyramidal system [in German]. *Klin Wochenschr*. 1960;38:1236-1239.
20. Schapira AHV, Chaudhuri KR, Jenner P. Non-motor features of Parkinson disease. *Nat Rev Neurosci*. 2017;18(7):435-450.
21. Gibb WRG, Lees AJ. Anatomy, pigmentation, ventral and dorsal subpopulations of the substantia nigra, and differential cell death in Parkinson's disease. *J Neurol Neurosurg Psychiatry*. 1991;54(5):388-396.
22. Blesa J, Trigo-Damas I, Dileone M, del Rey NLG, Hernandez LF, Obeso JA. Compensatory mechanisms in Parkinson's disease: circuits adaptations and role in disease modification. *Exp Neurol*. 2017;298(pt B):148-161.
23. Gregory S, Long JD, Klöppel S, et al. Operationalizing compensation over time in neurodegenerative disease. *Brain*. 2017;140(4):1158-1165.
24. Wilson H, Niccolini F, Pellicano C, Politis M. Cortical thinning across Parkinson's disease stages and clinical correlates. *J Neurol Sci*. 2019;398:31-38.
25. Wang L, Zhou C, Cheng W, et al. Dopamine depletion and subcortical dysfunction disrupt cortical synchronization and metastability affecting cognitive function in Parkinson's disease. *Hum Brain Mapp*. 2022;43(5):1598-1610.
26. Liu FT, Ge JJ, Wu JJ, et al. Clinical, dopaminergic, and metabolic correlations in Parkinson disease: a dual-tracer PET study. *Clin Nucl Med*. 2018;43(8):562-571.
27. Wang L, Cheng W, Rolls ET, et al. Association of specific biotypes in patients with Parkinson disease and disease progression. *Neurology*. 2020;95(11):e1445-e1460.
28. Cabeza R, Albert M, Belleville S, et al. Maintenance, reserve and compensation: the cognitive neuroscience of healthy ageing. *Nat Rev Neurosci*. 2018;19(11):701-710.
29. Marek K, Jennings D, Lasch S, et al. The Parkinson Progression Marker Initiative (PPMI). *Prog Neurobiol*. 2011;95(4):629-635.
30. Hughes AJ, Daniel SE, Kilford L, Lees AJ. Accuracy of clinical diagnosis of idiopathic Parkinson's disease: a clinico-pathological study of 100 cases. *J Neurol Neurosurg Psychiatry*. 1992;55(3):181-184.
31. CAT: A Computational Anatomy Toolbox for SPM. Accessed November 19, 2019.neuro.uni-jena.de/cat/.
32. Chung MK, Worsley KJ, Paus T, et al. A unified statistical approach to deformation-based morphometry. *Neuroimage*. 2001;14(3):595-606.
33. Parashos SA, Luo S, Biglan KM, et al. Measuring disease progression in early Parkinson disease the national institutes of health exploratory trials in Parkinson disease (NET-PD) experience. *JAMA Neurol*. 2014;71(6):710-716.
34. Marek K, Chowdhury S, Siderowf A, et al. The Parkinson's progression markers initiative (PPMI)—establishing a PD biomarker cohort. *Ann Clin Transl Neurol*. 2018;5(12):1460-1477.
35. Wu P, Wang J, Peng S, et al. Metabolic brain network in the Chinese patients with Parkinson's disease based on 18F-FDG PET imaging. *Park Relat Disord*. 2013;19(6):622-627.
36. Hawrylycz MJ, Lein ES, Guillozet-Bongaarts AL, et al. An anatomically comprehensive atlas of the adult human brain transcriptome. *Nature*. 2012;489(7416):391-399.
37. Arnatkevičiūtė A, Fulcher BD, Fornito A. A practical guide to linking brain-wide gene expression and neuroimaging data. *Neuroimage*. 2019;189:353-367.
38. Chen J, Bardes EE, Aronow BJ, Jegga AG. ToppGene Suite for gene list enrichment analysis and candidate gene prioritization. *Nucleic Acids Res*. 2009;37(Web Server issue):W305-W311.
39. ToppGene Suite. Accessed September 2020.toppgene.cchmc.org/.
40. Zeighami Y, Ulla M, Iturria-Medina Y, et al. Network structure of brain atrophy in de novo Parkinson's disease. *Elife*. 2015;4:e08440.
41. Filippi M, Canu E, Donzuso G, et al. Tracking cortical changes throughout cognitive decline in Parkinson's disease. *Mov Disord*. 2020;35(11):1987-1998.
42. Rolls ET, Joliot M, Tzourio-Mazoyer N. Implementation of a new parcellation of the orbitofrontal cortex in the automated anatomical labeling atlas. *Neuroimage*. 2015;122:1-5.
43. Seibyl JP, Marchek KL, Quinlan D, et al. Decreased single-photon emission computed tomographic {123I}β-CIT striatal uptake correlates with symptom severity in Parkinson's disease. *Ann Neurol*. 1995;38(4):589-598.
44. Xiang X, Wind K, Wiedemann T, et al. Microglial activation states drive glucose uptake and FDG-PET alterations in neurodegenerative diseases. *Sci Transl Med*. 2021;13(615):eabe5640.
45. Johnson ECB, Dammer EB, Duong DM, et al. Large-scale proteomic analysis of Alzheimer's disease brain and cerebrospinal fluid reveals early changes in energy metabolism associated with microglia and astrocyte activation. *Nat Med*. 2020;26(5):769-780.
46. Chang D, Nalls MA, Hallgrímsdóttir IB, et al. A meta-analysis of genome-wide association studies identifies 17 new Parkinson's disease risk loci. *Nat Genet*. 2017;49(10):1511-1516.
47. Pagonabarraga J, Tinazzi M, Caccia C, Jost WH. The role of glutamatergic neurotransmission in the motor and non-motor symptoms in Parkinson's disease: clinical cases and a review of the literature. *J Clin Neurosci*. 2021;90:178-183.
48. Nandhagopal R, Kuramoto L, Schulzer M, et al. Longitudinal evolution of compensatory changes in striatal dopamine processing in Parkinson's disease. *Brain*. 2011;134(pt 11):3290-3298.
49. Shine JM, Bell PT, Matar E, et al. Dopamine depletion alters macroscopic network dynamics in Parkinson's disease. *Brain*. 2019;142(4):1024-1034.
50. Arkadir D, Bergman H, Fahn S. Redundant dopaminergic activity may enable compensatory axonal sprouting in Parkinson disease. *Neurology*. 2014;82(12):1093-1098.
51. Schweitzer JS, Song B, Herrington TM, et al. Personalized iPSC-derived dopamine progenitor cells for Parkinson's disease. *N Engl J Med*. 2020;382(20):1926-1932.
52. Kim R, Park S, Yoo D, Jun JS, Jeon B. Association of physical activity and APOE genotype with longitudinal cognitive change in early Parkinson disease. *Neurology*. 2021;96(19):e2429-e2437.

# Association of Structural Measurements of Brain Reserve With Motor Progression in Patients With Parkinson Disease

Linbo Wang, Ping Wu, Peter Brown, et al.

*Neurology* 2022;99;e977-e988 Published Online before print June 6, 2022
DOI 10.1212/WNL.0000000000200814